



Diagnosis and Staging of Pancreatic Cancer: Imaging Evaluations—Pancreatic Protocol CT and MRI, PET-CT

Sanaz Javadi, Vincenzo Wong,
Juan J. Ibarra Rovira, Priya Bhosale, and Eric Tamm

Computed Tomography

Computed tomography (CT) is the imaging modality of choice for detection and staging of pancreatic cancer due to its high spatial resolution and the ability to produce multiplanar reformats. The proper imaging protocol and technique is crucial for these purposes.

CT Protocol

Recent recommendations from the National Comprehensive Cancer Network, based on consensus publications written by members of the

American Pancreatic Association including radiologists from the Society of Abdominal Radiology, provide detailed instructions to optimize imaging with computed tomography [1]. These recommendations include the following for a CT examination optimized for detection, characterization, and staging of a pancreatic mass that may be a pancreatic tumor. Intravenous iodinated contrast should be injected rapidly at a rate of approximately 3–5 mL per second. Imaging should be obtained during the phase of peak pancreatic parenchymal enhancement, typically 40–50 s following the start of injection of intravenous contrast, followed then by a second phase, a portal venous phase, at 65–70 s after the start of contrast injection. The pancreatic parenchymal phase facilitates imaging of the primary tumor, as well as arterial anatomy, while the portal venous phase facilitates visualization of venous structures and the detection of liver metastases. Neutral contrast, such as water, should be utilized. Images should be obtained at the thinnest slice profile possible, preferably submillimeter, to allow for reconstructions in the axial, coronal, and sagittal planes at a 2–3 mm slice thickness to facilitate visualization of the relationship of tumor to vessels (Fig. 5.1). Dual energy imaging techniques, in which X-ray beams of two different energies are utilized at the same time, have been shown to improve the visibility of pancreatic tumors, particularly low, 40–50 keV monochromatic energy images as well as iodine material density images which empha-

S. Javadi (✉)
Diagnostic Radiology, University of Texas MD
Anderson Cancer Center, Houston, TX, USA
e-mail: sanaz.javadi@mdanderson.org

V. Wong · J. J. Ibarra Rovira · P. Bhosale
Abdominal Imaging, University of Texas MD
Anderson Cancer Center, Houston, TX, USA
e-mail: vk Wong@mdanderson.org;
jjibarra@mdanderson.org

P. Bhosale
Abdominal Imaging, The University of Texas MD
Anderson Cancer Center, Houston, TX, USA
e-mail: [Priya.bhosale@mdanderson.org](mailto: Priya.bhosale@mdanderson.org)

E. Tamm
Department of Abdominal Radiology, University of
Texas MD Anderson Cancer Center,
Houston, TX, USA
e-mail: [etamm@mdanderson.org](mailto: etamm@mdanderson.org)

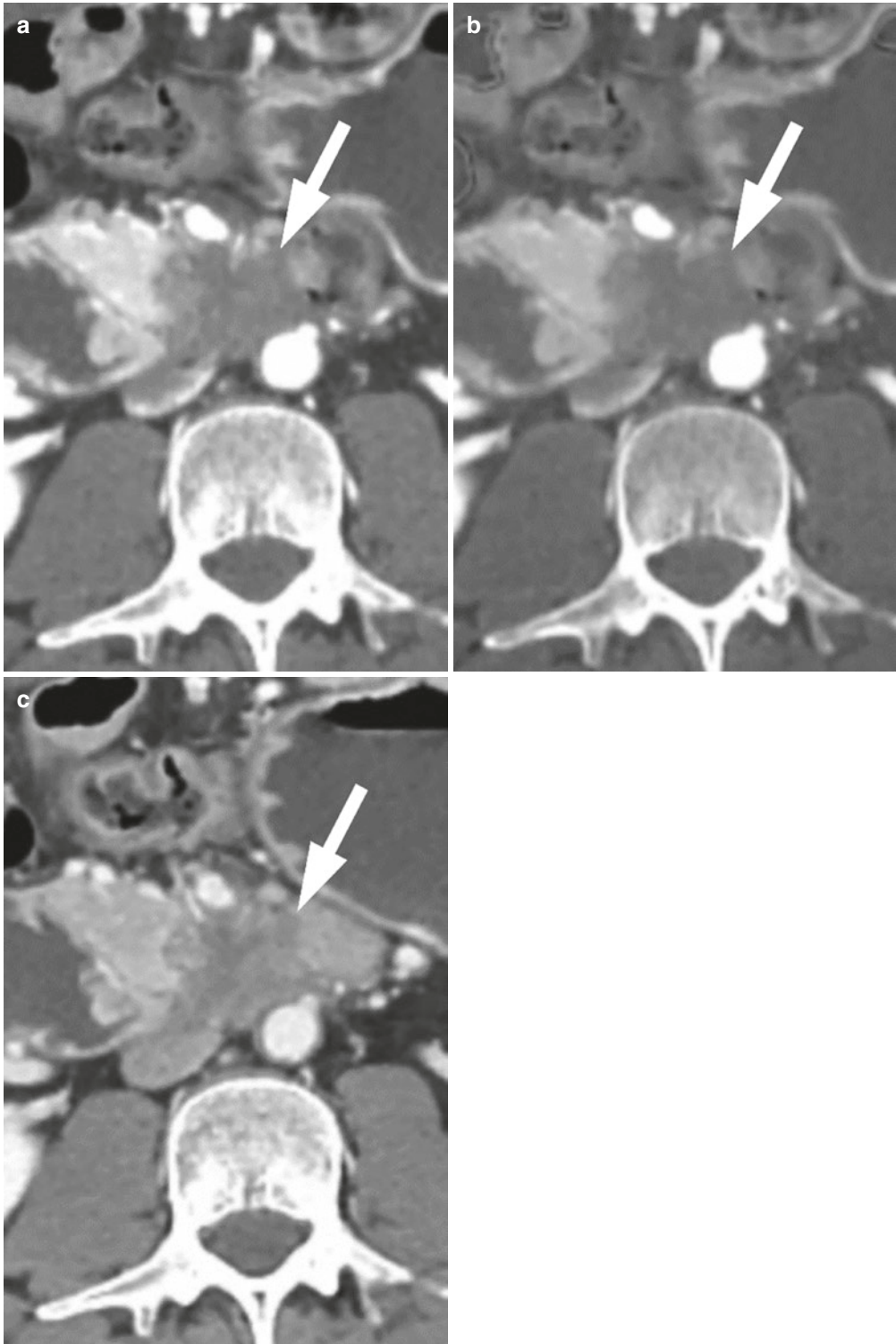


Fig. 5.1 Pancreatic head mass (white arrow) as seen on the (a) late arterial phase, (b) late arterial phase on iodine material density dual energy image, and (c) late

arterial phase. Note how boundaries of tumor and difference between tumors are better seen on late arterial phase and particularly the iodine material density image

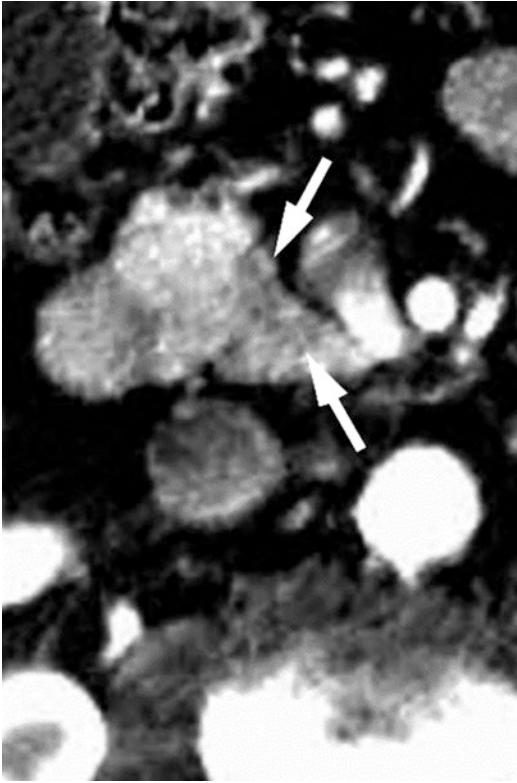


Fig. 5.2 Medial hypodense pancreatic head lesion (white arrows), biopsy proven chronic pancreatitis. Lesion remained stable over the course of multiple examinations

size the presence of iodinated contrast (Fig. 5.1) [2, 3]. Alternatively, imaging can be done using a low kVp (80–100kVp) technique to improve contrast, though limitations on tube output may constrain imaging with regard to patient size [4, 5].

Diagnosis

Pancreatic ductal adenocarcinoma (PDAC) on contrast-enhanced CT typically has the appearance of a solid mass. This is variably hypodense to background pancreas on the pancreatic parenchymal phase of enhancement (late arterial phase) (Fig. 5.1). The sensitivity for the detection of tumor on multidetector CT has been reported to be approximately 86–97% when considering tumors of all sizes, but decreases to a sensitivity of 77% for tumors under 2 cm [6–9]. Dual energy imaging techniques have been shown to improve

the conspicuity of primary tumors, particularly low keV monochromatic energy images, approximately 40–50 keV, and iodine material density images, the latter emphasizing the differences in contrast enhancement between tumor and background pancreas [2, 3]. However, even with biphasic imaging, pancreatic tumors can be isodense to the background pancreas. A study utilizing multidetector CT noted an incidence of 11% for isoattenuating tumors even during the phase of peak pancreatic enhancement [10].

In the case of such isoattenuating tumors, it is important to be aware of secondary signs, which may be the only indicator(s) present. These include atrophic pancreatic parenchyma within the upstream pancreas, abnormal mass effect including regional pancreatic enlargement, abnormal pancreatic contour, and abnormalities of the pancreatic and/or common bile duct. Abnormalities of the main pancreatic duct include an interrupted or obstructed main pancreatic duct [10]. Studies have shown that dilatation of the main pancreatic duct with cut-off can be seen in nearly half of cases as distant as 2–18 months prior to establishing a clinical diagnosis of pancreatic cancer [11].

Differential Diagnosis

One of the challenges is the broad differential diagnosis for a hypodense or isodense pancreatic mass, the primary concern always being the possibility of pancreatic ductal adenocarcinoma. For this reason, tissue sampling is almost always needed to guide further management. The etiologies that will be covered include both inflammatory and neoplastic.

The primary inflammatory considerations are forms of chronic pancreatitis, both conventional and autoimmune varieties. Histopathologically, conventional (non-autoimmune) chronic pancreatitis is characterized by parenchymal destruction with replacement by fibrotic tissue classically resulting in an atrophied pancreas [12, 13]. However, chronic pancreatitis can also manifest as a focal mass (30%) (Fig. 5.2) causing features that mimic pancreatic ductal adenocarcinoma, including duct obstruction [13, 14]. Overall, CT

has been reported to have a specificity of only 70% when discriminating between mass-forming chronic pancreatitis and pancreatic ductal adenocarcinoma [15]. Another challenge is that patients with chronic pancreatitis are at risk for developing pancreatic ductal adenocarcinoma [16]. For this reason, even if a biopsy of such a mass is negative for malignancy and is indicative of pancreatitis, close observation, and consideration for re-biopsy is advised because of the issues like sampling errors and potential future development of cancer.

Autoimmune pancreatitis, a manifestation of a related systemic disease, has an average age of onset of 60 years, but can affect a wide age range [17]. It manifests as two main types: Type 1, a predominantly lobular inflammatory manifestation with a typically diffuse fusiform appearance in which most patients develop an elevated serum IgG4 level, and Type 2, histopathologically associated with granulomas centered about ducts, commonly forming a mass, and only rarely mounting an elevated serum IgG4 level [17].

The neoplastic differential diagnosis for pancreatic ductal adenocarcinoma includes primary and metastatic tumors.

Primary pancreatic neuroendocrine tumors, while classically hyperenhancing on the pancreatic parenchymal phase, can be isoenhancing or even hypoenhancing on the pancreatic parenchymal phase; hypoenhancing variants were also identified to have poorer prognosis with higher rates of nodal and liver metastases [18].

Primary pancreatic lymphoma is rare, but secondary pancreatic involvement has been reported in up to 30% of cases of non-Hodgkin lymphoma [19]. The appearance can be variable, including diffuse pancreatic involvement as well as manifesting as one or more solid masses (Fig. 5.3), with or without obstruction of the main pancreatic duct [19].

Several extra-pancreatic primary tumors can metastasize to the pancreas. These include those originating in the breast, colon (Fig. 5.4), kidneys, lungs, and prostate. Sarcomas, melanoma, and bowel carcinoid tumors can also metastasize to the pancreas. These lesions can show a variety of enhancement patterns, ranging from hyper- to



Fig. 5.3 Pancreatic neck hypodense mass (white arrows), confirmed as lymphoma, encasing the common hepatic artery (white arrowhead). Atrophic upstream pancreas (thick white arrow)

hypoenhancement. While the presence of multiple solid lesions is a useful indicator for metastatic disease or lymphoma, metastatic disease to the pancreas can often manifest as a solitary lesion. For this reason, the possibility of metastatic disease, rather than solely primary pancreatic cancer, should be considered in the setting of a known extra-pancreatic primary. Biopsy and tools such as immunohistochemistry are often helpful.

Staging

The American Joint Committee on Cancer (AJCC) provides staging criteria for pancreatic adenocarcinoma that follows the tumor/node/metastasis (TNM) model. There are criteria within the TNM model that can only be obtained



Fig. 5.4 Metastatic colon cancer mass (white arrows) involving the pancreatic head and central mesenteric vessels, with 360° encasement of the superior mesenteric artery (black arrowhead)

after surgery, for example, nodal staging. Thus, the TNM system is more tailored for stratification and prognostication rather than pre-operative evaluation. In 2016, the eighth edition of the American Joint Committee on Cancer (AJCC) Staging Manual was released which included updates on the staging of pancreatic cancer (Table 5.1). One important change was splitting pancreatic cancers into cancers of the endocrine pancreas and exocrine pancreas, which now use different staging systems. Primary tumor staging (T) was moved from a more descriptive-based to a more size-based system. Nodal staging (N) was changed to incorporate the number of positive lymph nodes.

T-staging is divided into four categories, T1–T4, based on tumor size and involvement of the celiac axis (CA), superior mesenteric artery (SMA), or common hepatic artery (CHA). A T1

tumor is defined as a tumor size ≤ 2 cm without involvement of the CA, SMA, or CHA. The eighth edition of the AJCC staging manual has further subcategorized T1 into T1a (tumor ≤ 0.5 cm), T1b (tumor >0.5 and < 1 cm), and T1c (tumor 1–2 cm). A T2 tumor is defined as a tumor >2 cm and ≤ 4 cm in greatest dimension without involvement of the CA, SMA, or CHA. A T3 tumor is defined as a tumor >4 cm without involvement of the CA, SMA, or CHA. Previously in the seventh edition of the AJCC Staging Manual, the T3 category was defined as a tumor that extends beyond the pancreas, regardless of size, but without involvement of the celiac axis or the superior mesenteric artery. However, extension beyond the pancreas may vary among pathologists and may not be reproducible. Additionally, the pancreas lacks a true capsule to delineate extension beyond the pancreas, and chronic pancreatitis can obliterate the pancreatic and peripancreatic interface which can contribute to difficulty in determining extension beyond the pancreas [20]. As a result, nearly all cases of PDAC could be classified as T3 disease based on extra-pancreatic according to the seventh edition [21]. The T4 category is assigned to tumors that involve the celiac axis, superior mesenteric artery, or common hepatic artery, regardless of size. One change in the definition of a T4 tumor between the seventh and eighth editions is removal of the phrase “unresectable primary tumor” because resectability varies among institutions.

N-staging is divided into three categories. N0 refers to no regional lymph node metastasis. N1 is defined as metastasis to 1 to 3 regional lymph nodes. N2 is defined as metastasis to 4 or more regional lymph nodes. N-staging was changed to incorporate the number of positive lymph nodes which has shown better prognostication for survival. In one study, 5 year survival rates for N0 status were 35.6%, N1 status was 20.8%, and N2 status was 10.9% ($P < 0.01$) [22].

M-staging remains unchanged between the seventh and eighth editions. M0 is defined as no distant metastases are present. M1 is defined as distant metastases are present.

To address tumor resectability, there are different classification systems from different insti-

Table 5.1 American Joint Committee on Cancer (AJCC) Staging Manual for pancreatic cancer comparing seventh and eighth editions

	AJCC Staging Manual (seventh edition, 2010)	AJCC Staging Manual (eighth edition, 2016)
Primary tumor (T)	TX primary tumor cannot be assessed	TX primary tumor cannot be assessed
	Tis carcinoma in situ	Tis carcinoma in situ
	T1 tumor limited to the pancreas, ≤2 cm in greatest dimension	T1 tumor ≤2 cm in greatest dimension T1a tumor ≤0.5 cm in greatest dimension T1b tumor > 0.5 and < 1 cm in greatest dimension T1c tumor 1–2 cm in greatest dimension
	T2 tumor limited to the pancreas, >2 cm in greatest dimension	T2 tumor >2 cm and ≤ 4 cm in greatest dimension
	T3 tumor extends beyond the pancreas but without involvement of the celiac axis or the superior mesenteric artery	T3 tumor >4 cm in greatest dimension
	T4 tumor involves the celiac axis or the superior mesenteric artery (unresectable primary tumor)	T4 tumor involves celiac axis, superior mesenteric artery, or common hepatic artery, regardless of size
Node status (N)	NX regional lymph nodes cannot be assessed	NX regional lymph nodes cannot be assessed
	N0 no regional lymph node metastasis	N0 no regional lymph node metastasis
	N1 metastasis to regional nodes	N1 metastasis to 1 to 3 regional nodes
		N2 metastasis to 4 or more regional nodes
Distant metastasis (M)	M0 no distant metastasis present	M0 no distant metastasis present
	M1 distant metastasis present	M1 distant metastasis present

Table 5.2 Comparison of resectability across different organizations

Vascular Involvement	NCCN 2019	MDACC	AHPBA/SSAT/SSO
SMA ≤ 180°	Borderline	Borderline	Borderline
SMA > 180°	Unresectable	Unresectable	Unresectable
CA ≤ 180°	Borderline	Borderline	Unresectable
CA > 180°	Head/uncinate: Unresectable Body/tail: Borderline if aorta and GDA uninvolved to allow for modified Appleby procedure	Unresectable	Unresectable
CHA abutment or short segment encasement	Borderline	Borderline	Borderline
PV or SMV > 180° or ≤ 180° with contour irregularity or thrombosis with reconstruction possible	Borderline	Borderline	Borderline

tutions and societies. MD Anderson Cancer Center (MDACC) was the first to publish such a system [23]. Other classifications include the National Comprehensive Cancer Network (NCCN), as well as the joint consensus between the Americas Hepato-Pancreato-Biliary Association (AHPBA), Society for Surgical Oncology (SSO), and Society for Surgery of the

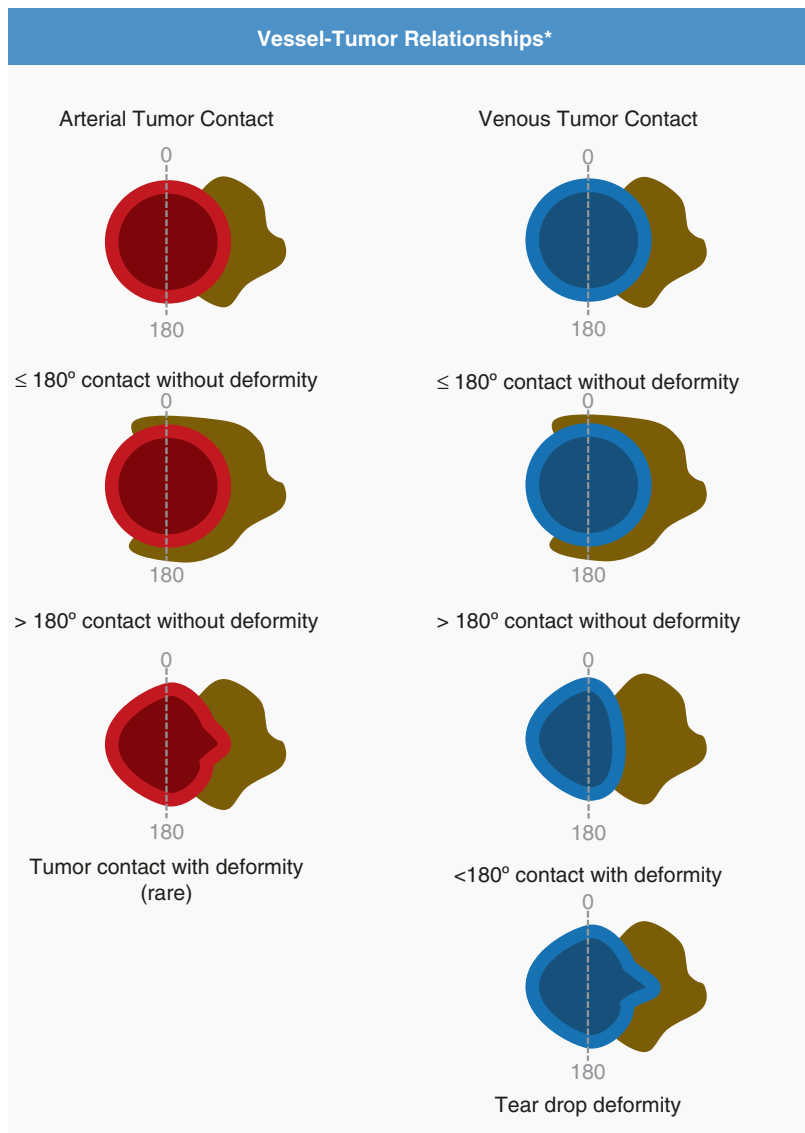
Alimentary Tract (SSAT). Common to the classification systems, pancreatic adenocarcinoma can be categorized as resectable, borderline resectable, and unresectable based on the presence or absence of distant metastatic disease and degree of artery and vein involvement by the tumor. These differences are highlighted in (Table 5.2).

The degree of vascular involvement of tumor is based on how much of the tumor contacts the surface of the involved vessel, from no contact to 360 degrees. This can be divided into tumors that have $\leq 180^\circ$ of contact with the vessel (abutment) and $>180^\circ$ of contact with the vessel (encasement). One prospective study evaluated the degree of vascular involvement on pre-operative CT in 25 patients who underwent resection or palliative surgery for PDAC. The authors found that $>180^\circ$ of involvement had a positive predictive value of 95% and negative predictive value of 92% for unresectability of the tumor

from the vessel [24]. Deformities in the involved vessels such as a tear-drop deformity are other qualitative factors that help determine vascular involvement. A tear-drop deformity describes the shape of the vessel as it is pinched by the surrounding tumor which is indicative of vascular invasion regardless of the degree of tumor-vessel contact [24–26] (Fig. 5.5).

Resectable tumors are those without arterial tumor contact of the CA, SMA, or CHA, or venous tumor contact of the PV, SMV, or $\leq 180^\circ$ of involvement without venous contour deformity (Fig. 5.6).

Fig. 5.5 The degree of vascular involvement of tumor, based on how much of the tumor contacts the surface of the involved vessel (0–360°) [26]



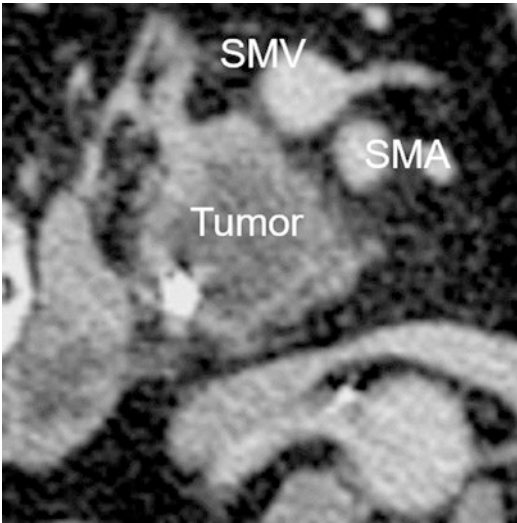


Fig. 5.6 The SMV and SMA are uninvolved by the pancreatic cancer. There is a clear fat plane between these vessels and the tumor, qualifying this as a resectable mass

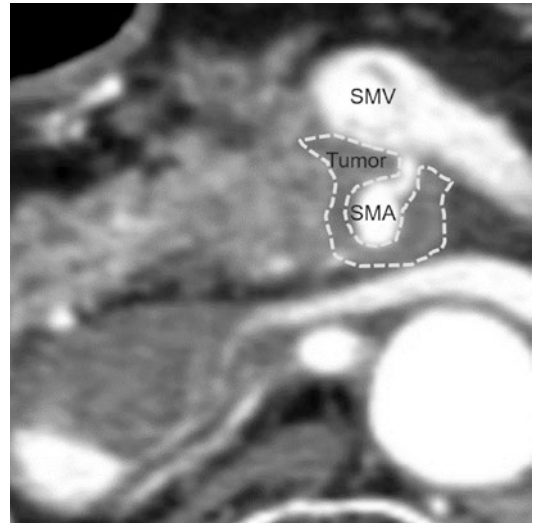


Fig. 5.7 The tumor contacts $>180^\circ$ of the SMA qualifying this as an unresectable mass

Unresectable tumors are those with distant metastatic disease including non-regional lymph node metastasis or locally advanced disease. Tumors involving $>180^\circ$ degrees of the CA or SMA are unresectable, as are those with venous involvement that do not allow for vascular reconstruction, or contact with the most proximal draining jejunal branch into the SMV (Fig. 5.7). AHPBA/SSAT/SSO guidelines define any tumor abutment ($\leq 180^\circ$) of the CA as unresectable.

Borderline resectable masses are those that have degrees of vascular involvement that fall in between the definition of resectable and unresectable disease. Tumors that show $>180^\circ$ of involvement of the SMV or PV, or those with $\leq 180^\circ$ of involvement with contour abnormality that are reconstructable are considered borderline resectable. Tumors that contact $\leq 180^\circ$ or with short segment encasement ($>180^\circ$) of the CHA or contact $\leq 180^\circ$ of the SMA are also borderline resectable (Fig. 5.8).

For borderline resectable tumors that undergo pre-operative therapy with chemotherapy or radiation, it is important to note that radiologic downstaging is rare after treatment. The imaging appearance of the tumor before treatment and

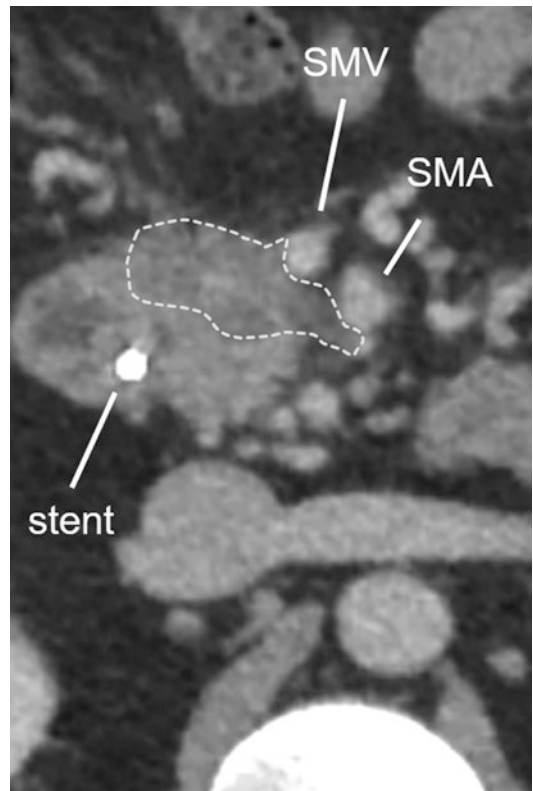


Fig. 5.8 The tumor contacts $\leq 180^\circ$ of the SMA and SMV, qualifying this as a borderline resectable mass

after treatment is unlikely to change based on RECIST criteria or alter the imaging appearance of vascular involvement. In a study by Katz et al. that evaluated borderline PDAC after neoadjuvant therapy, only 1 out of 129 patients showed a radiographic reduction in vascular involvement to improve their anatomic stage, while 15 out of 122 patients met criteria for treatment response by RECIST criteria. Despite the findings, R0 (margin-negative) resection was achieved in 81 out of the 101 patients that did not develop metastatic disease [27]. The median overall survival between patients that did not show a radiographic response to therapy was the same as those that did show a radiographic response [27].

The use of standardized reports and standardized language for pre-operative staging CT provides consistency for crucial information that helps to determine optimal management, as well as improve patient care across institutions. Standardized reports should include morphologic, arterial, venous, and extra-pancreatic findings. Under morphologic findings, one may describe tumor location (head, uncinate process, body, tail), size, appearance, pancreatic ductal and biliary ductal dilation. Arterial findings should include variant arterial anatomy, assessment of the CA, CHA, and SMA, and evaluation for soft tissue contact, hazy attenuation or stranding, vessel narrowing or contour abnormality. Venous findings should include assessment of the portal vein and SMV, documentation of thrombus and collaterals, and vessel narrowing or contour abnormality. Extra-pancreatic findings should include evaluation of nodes, liver lesions, peritoneal disease, ascites, and other sites of metastatic disease.

Positron Emission Tomography/ Computed Tomography

Positron emission tomography/computed tomography (PET/CT) imaging has been used to diagnose, stage, and follow up of pancreatic cancer. PET imaging uses the principle of tumor glycolysis to detect sites of disease and has been used as

a prognostic indicator. PET/CT integrates both, morphological and functional data, to compensate for some deficiencies from individual modalities (poor contrast resolution on CT imaging for small lesions and poor spatial resolution in PET imaging). Since the normal pancreas is not highly metabolic on PET, any region of increased radiotracer uptake should be considered abnormal.

PET/CT Protocol

The radiopharmaceutical tracer used in the diagnosis and management of the great majority of malignancies is 18-F-FDG (18-F-fluoro-2-deoxyglucose) which is administered intravenously; therefore, intravenous (IV) access must be obtained prior to examination. Dosage recommended by the International Commission on Radiological Protection (ICRP) is approximately 259 MBq (7 mCi) of FDG with variability between 290 s and 500 s MBq (8–15 mCi) in an adult patient [28, 29]. Since 18-F-FDG is an analog of glucose, 6–8 h of fasting is recommended prior to the examination. The blood glucose levels are tested and should be within normal limits (4–7 mmol/L) or at least less than 140 mg/dL. Patients are usually placed in a dark quiet room prior to the examination to limit physiologic uptake in the muscles. Once the tracer is injected, it has an initial physiologic distribution into the brain, heart, kidneys, and urinary tract within 60 min. Imaging is acquired 60 min post-injection. The images are acquired from head to toe, first with low dose CT images are obtained and then PET imaging [28]. The CT portion of the PET/CT may be performed with or without intravenous contrast; however, we do recommend using contrast, as it gives better anatomic delineation.

Diagnosis

PET has higher sensitivity in detection of pancreatic cancer (92%) than CT (87%) and MRI (69%); however, the specificity is much lower at

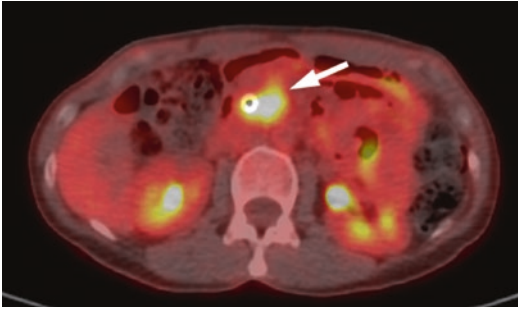


Fig. 5.9 Fused PET/CT image showing an avid mass in the head of the pancreas (arrow)

65% compared to 96% and 93% for CT and MRI, given that the FDG uptake can be seen in other malignancies affecting the pancreas like metastasis and inflammatory processes like acute pancreatitis and mass-forming chronic pancreatitis (Fig. 5.9) [30]. These findings correlate with previously reported meta-analysis studies [31–34].

Staging

PET/CT is limited in local tumor (T) staging of the pancreatic cancer due to the common use of un-enhanced CT component as well as relatively poor spatial resolution when compared to multiphase enhanced CT. The extent of tumor involvement of peripancreatic vessels and organs cannot be well evaluated with PET/CT, thus, requiring more accurate evaluation with another modality including multiphase CT, MRI, or EUS. If the patient is eligible for surgical treatment based on prior CT and/or diagnostic laparoscopy, it is preferred that the study is performed 1–2 weeks before scheduled surgery [35].

Nodal (N) disease is one of the most important prognostic factors affecting management in patients with pancreatic cancer. Accurate detection of metastatic lymph nodes is of extreme importance, since any positive lymph node outside of the surgical field is considered M1 and may preclude surgical resection (Fig. 5.10). On CT and MRI, the detection of metastatic lymph nodes is based on enlarged size (short axis size >1 cm); however, benign reactive lymph nodes

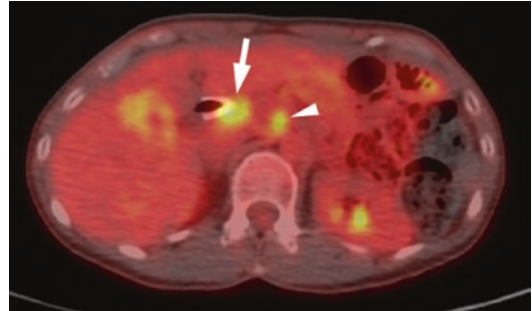


Fig. 5.10 Fused PET/CT image showing the presence of an FDG avid celiac lymph node (arrowhead) with an FDG avid pancreatic head mass (arrow)

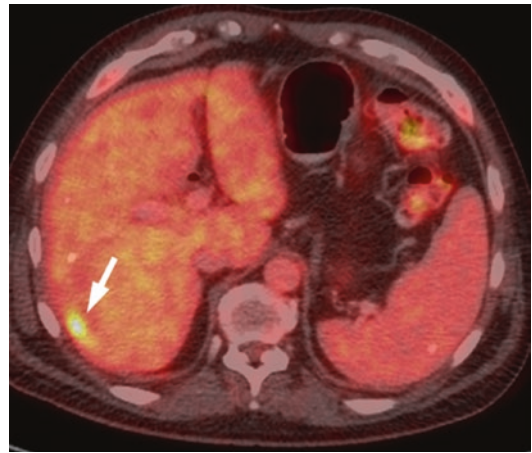


Fig. 5.11 Fused PET/CT image demonstrating an FDG avid liver metastasis (arrow) in a patient with pancreatic cancer

can also be enlarged, confounding the accurate staging. In particular, reactive lymphadenopathy can be seen after biopsy or biliary instrumentation. PET can also underestimate tumor involvement in small lymph nodes <0.5 cm due to its limited spatial resolution (5–8 mm). However, the odds of detection of these micrometastases are improved when there is significant elevation of CA 19–9 level and SUVmax of the primary tumor, especially when CA 19–9 values are above 240 U/mL and primary tumor SUVmax level is over 7.2 \pm 2.6 [36].

Distant metastatic (M) disease in PDAC is frequently detected in the liver, peritoneum, lungs, and bones (Fig. 5.11). PET/CT has shown to be superior in detecting bone metastasis. The

advantage of PET is the detection of distant metastasis. PET/CT was shown to be superior to PET alone in detection of hepatic metastasis (82% versus 67%, respectively). It is also superior to CT plus endoscopic ultrasound (EUS) in borderline resectable cases for detection of metastatic disease, sparing these patients from unnecessary surgeries. Several studies reported that PET resulted in staging changes in 27% and management changes in up to 11% of the patients [29, 33].

Treatment Response

PET is valuable in evaluation of treatment response or detection of progression of disease, since metabolic activity changes precede tumor size changes (Fig. 5.12). Prior prospective trials demonstrated that lower baseline and post-chemotherapy SUVmax on PET was predictive of histological response. Also, SUVmax, metabolic tumor volume (MTV), and total lesion glycolysis (TLG) may be significant prognostic factors [37]. In the neoadjuvant setting, if there is progression of disease, patients can be spared from undergoing an unnecessary operation with a high morbidity and in the adjuvant setting, an adjustment or change of chemotherapy regimen can be performed based on changes in metabolic activity of the tumor on PET/CT.

Detection of Recurrent Disease

Contrast-enhanced CT is the most frequently used modality for detection of recurrent disease. But in certain cases, including patients who cannot undergo contrast-enhanced CT due to renal failure or contrast allergy or in patients with suspected recurrence due to mild or equivocal elevations of CA 19-9 without morphologic signs of disease recurrence; PET/CT has clear value, detecting metabolically active disease. PET/CT has sensitivity of 91%, specificity of 100%, and accuracy of 92% for detection of recurrent pancreatic cancer [38].

Magnetic Resonance Imaging

MRI Protocol

MRI for diagnosis and staging of pancreatic cancer may be performed on a 1.5 or 3.0 Tesla gradient systems using cardiac 16 channel coils phased-array torso coils to improve the signal-to-noise ratio. An MRI protocol should include a single-shot fast spin-echo (SSFSE) sequence in the coronal plane, an axial fat-saturated T2 FSE sequence, a T1 gradient echo (GRE) fat-saturated sequence, and a post-contrast 3D dynamic GRE sequences in arterial, portal, and delayed phases. Diffusion weighted imaging (DWI) has been

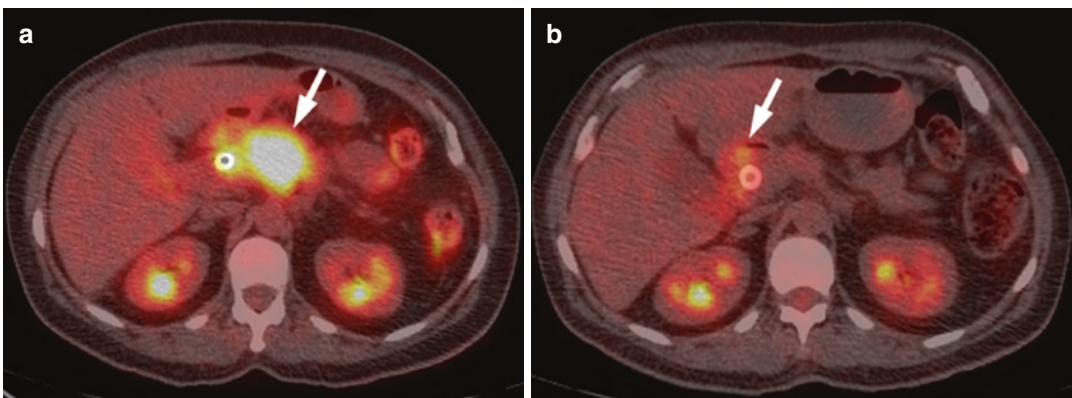


Fig. 5.12 Fused PET/CT images demonstrating (a) the pre-adjvant therapy scan with FDG avid pancreatic head mass (arrow) and (b) decreased FDG avidity of the pan-

creatic head mass (arrow) suggestive of a favorable response to treatment in a patient with advanced pancreatic cancer

used in assessment of pancreatic cancers. Coronal and axial magnetic resonance cholangiopancreatography (MRCP) images are usually obtained. Fast imaging employing steady-state acquisition (FIESTA) or true fast imaging with steady-state free precession (Tru-FISP) images are performed to assess the vessels. The typical MRCP techniques involve fluid-sensitive sequences such as thin-section T2-weighted single-shot fast spin-echo (HASTE/SSFSE) and thick-slab T2-weighted half-Fourier SSFSE MRCP and 3D respiratory-triggered or navigator-triggered techniques.

Diagnosis

Currently, MR is used as a “problem-solving” tool in patients with an inconclusive CT diagnosis or in suspected masses without contour deformity of the pancreas. MR can also be used for pre-operative staging in patients who are allergic to iodinated contrast agents or have renal insufficiency.

MRI has an excellent soft tissue resolution and can detect signal intensity changes within the pancreas. The normal pancreas has a high signal intensity on T1-weighted fat-suppressed sequences due to acinar proteins which shorten the T1 values of the normal gland [39]. The normal pancreas enhances maximally during the

arterial phase of contrast enhancement [40]. PDACs are low in signal on the precontrast and the post-contrast images compared to the pancreatic parenchyma due to presence of fibrous stroma [39, 41]. On delayed phase, more than 1 min delay in enhancement may result in invisibility of pancreatic cancer, since the contrast diffuses through the capillaries and tumor becomes similar in signal to that of the pancreatic parenchyma [39]. However, it should be noted that differentiating small PDAC from focal chronic pancreatitis might be very difficult or impossible [42]. Both focal chronic pancreatitis and PDAC can appear as focal hypointense masses with associated dilatation of common bile duct and main pancreatic duct (double-duct sign). Both conditions may also demonstrate ductal strictures, infiltration of the adjacent fat, arterial encasement, or venous obstruction [43]. There are often no distinguishing features on T1- and T2-weighted MR imaging [44]. Specific imaging features that favor an inflammatory mass are non-dilated or smoothly tapering pancreatic and bile ducts coursing through the mass (“duct-penetrating” sign) [45], irregularity of the pancreatic duct, and the presence of pancreatic calcifications. In contrast, a smoothly dilated pancreatic duct with an abrupt interruption prior to the ampulla favors the diagnosis of cancer (Fig. 5.13). Other feature that favors cancer is a mass at the site of obstruction resulting in distal

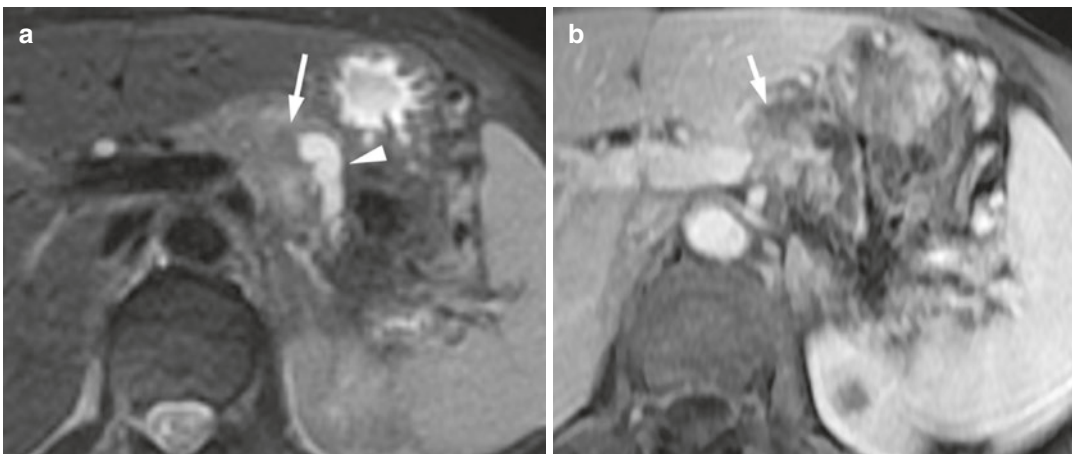


Fig. 5.13 (a) Axial T2 weighted MR image demonstrates dilated pancreatic duct (arrowhead) with abrupt cut off due to pancreatic cancer (arrow) and (b) corresponding

post-contrast MR image demonstrates a hypoenhancing mass (arrow) at the location of ductal cut off consistent with pancreatic cancer

atrophy of the pancreas [46]. A mass causing upstream chronic pancreatitis can sometimes be detected on early phase dynamic gadolinium-enhanced images. The cancer sometimes is seen as a focal hypointense mass relative to the hypoenhancing region of chronic pancreatitis on early gadolinium-enhanced images [46]. The combined MRI features of a focal pancreatic mass, pancreatic duct dilatation, and parenchymal atrophy are highly suggestive of ductal adenocarcinoma [42].

Approximately less than 50% of patients with pancreatic adenocarcinomas exhibit mildly hyperintense signal intensity on T2-weighted images [47]. The T2 signal intensity of PDAC may depend on the amount of desmoplastic reaction within the tumor and the degree of intratumoral necrosis as necrotic tumor may have a high T2 signal intensity. On MRCP, a double-duct sign is the common indirect sign which suggests presence of a pancreatic neoplasm, where the pancreatic duct and the common bile duct are both obstructed by the tumor [48]. A study reported a specificity of 97% and a sensitivity of 84% for MRCP images in the detection of pancreatic adenocarcinoma based on these findings [49]. On DWI, the PDAC demonstrates diffusion restriction and has a high signal intensity relative to the surrounding pancreatic tissue. Apparent diffusion coefficient (ADC) is a calculated value from a DWI sequence. One study showed that ADC values were able to differentiate pancreatic cancer (1.44 ± 0.20), compared to that of normal pancreas (1.90 ± 0.06) and tumor-associated chronic pancreatitis (2.31 ± 0.18) [50]. The sensitivity and specificity of MRI including T1-weighted 3D-GRE sequences for differentiating pancreatic carcinoma from chronic pancreatitis were 93% (13/14) and 75% (6/8), respectively [51].

Staging

Currently, complete resection provides the only potential cure for pancreatic adenocarcinomas. Classic contraindications for resection include involvement of the celiac axis, SMA encasement and organ invasion other than the duodenal, and

mesenteric infiltration. 3D Dynamic post-contrast T1 weighted imaging is a valuable tool to assess vascular encasement [47, 48] and can help in local staging of pancreatic cancer. The tumor in the pancreatic head can spread into the root of the mesentery, along the left jejunal vascular branches and the common hepatic artery resulting in unresectable tumor [52]. These findings can be well visualized on the post-contrast T1 weighted sequence or the FIESTA/tru-FISP sequences.

Liver is the most common site of distant metastasis in pancreatic cancer. Hepatic metastases from pancreatic cancers are low in signal intensity relative to the hepatic parenchyma on both fat-saturated and non-fat-saturated T1 weighted images. They are slightly hyperintense relative to the hepatic parenchyma on T2 weighted images during the short TE (time to echo) sequence and demonstrate irregular rim enhancement on the arterial phase. Signal intensity may be low in the center of the lesion because of the primary cancer's desmoplastic nature. Transient, ill-defined, peritumoral enhancement in the hepatic parenchyma may be present on the arterial phase of contrast enhancement. Perilesional enhancement is typically wedge-shaped and is usually present in small, hypervascular, and subcapsular liver metastases; these metastases are observed in more than 80% of the patients and may be the only site of metastases in up to 20% of the patients [53, 54]. Since the patients with pancreatic cancer frequently undergo biliary procedures and biopsies, they are prone to develop cholangitis and hepatic abscesses which can mimic metastasis. Asymptomatic focal cholangitis may present as a new hepatic lesion with restricted diffusion similar to metastasis. Hepatic abscesses tend to have T2 hyperintense signal with peripheral rim enhancement and would resolve following antibiotic therapy [55].

Assessment for metastatic lymph nodes may be difficult on MRI. On any cross-sectional imaging modality metastases to the lymph nodes are based on size. Lymph nodes >1 cm in the short axis are considered metastatic. However benign lymph nodes can also be enlarged leading to a

false negative diagnosis, similarly lymph nodes containing micrometastases may be of a normal size. Lymph nodes, which are centrally necrotic and have a high signal on the T2 weighted images, may be considered metastatic and this feature has a high specificity.

Assessment of Recurrent Cancer

Local recurrence post-surgery may appear as infiltrating soft tissue mass on the post-contrast T1 weighted sequence. The soft tissue thickening may be present along the vessels and the nerves specifically posterior to the SMA and SMV, at the surgical margin. Differentiating between tumor recurrence and post-inflammatory stranding may be difficult to diagnose in the early postoperative period. Recurrent tumor in the surgical bed can infiltrate into the adjacent stomach and the jejunal loops and along the hepatico-jejunostomy, causing biliary obstruction. The tumor markers will be elevated in the setting of recurrent disease whereas will be normal when the soft tissue thickening just represents fibrosis or granulation tissue [56].

Conclusion

Imaging plays a significant role in diagnosis, staging, and follow-up of pancreatic cancer. There are several entities including mass-forming focal pancreatitis, autoimmune pancreatitis, neuroendocrine tumor, or metastasis that can mimic pancreatic cancer. Each imaging modality has strengths and weaknesses for detection, staging, and follow-up of pancreatic cancer. CT is the main and most common imaging modality for evaluation and staging of pancreatic cancer. PET/CT can be used for detection and follow-up but is less frequently used for staging. MRI is mostly used for problem-solving and evaluation of hepatic lesions. Overall, pancreatic cancer should be evaluated with appropriate imaging in conjunction with tumor marker and clinical presentation of the patient. In some cases, multiple imaging modalities are needed for thorough evaluation of the patient.

References

1. Tempero MA. NCCN guidelines updates: pancreatic cancer. *J Natl Compr Canc Netw*. 2019;17(5.5):603.
2. Beer L, et al. Objective and subjective comparison of virtual monoenergetic vs. polychromatic images in patients with pancreatic ductal adenocarcinoma. *Eur Radiol*. 2019;29(7):3617–25.
3. Bhosale P, et al. Quantitative and qualitative comparison of single-source dual-energy computed tomography and 120-kVp computed tomography for the assessment of pancreatic ductal adenocarcinoma. *J Comput Assist Tomogr*. 2015;39(6):907–13.
4. Zamboni GA, et al. Single-energy low-voltage arterial phase MDCT scanning increases conspicuity of adenocarcinoma of the pancreas. *Eur J Radiol*. 2014;83(3):e113–7.
5. Macari M, et al. Dual-source dual-energy MDCT of pancreatic adenocarcinoma: initial observations with data generated at 80 kVp and at simulated weighted-average 120 kVp. *AJR Am J Roentgenol*. 2010;194(1):W27–32.
6. Fletcher JG, et al. Pancreatic malignancy: value of arterial, pancreatic, and hepatic phase imaging with multidetector row CT. *Radiology*. 2003;229(1):81–90.
7. Agarwal B, et al. Endoscopic ultrasound-guided fine needle aspiration and multidetector spiral CT in the diagnosis of pancreatic cancer. *Am J Gastroenterol*. 2004;99(5):844–50.
8. DeWitt J, et al. EUS-guided FNA of pancreatic metastases: a multicenter experience.[see comment]. *Gastrointest Endosc*. 2005;61(6):689–96.
9. Bronstein YL, et al. Detection of small pancreatic tumors with multiphase helical CT. *AJR Am J Roentgenol*. 2004;182(3):619–23.
10. Prokesch RW, et al. Isoattenuating pancreatic adenocarcinoma at multi-detector row CT: secondary signs. *Radiology*. 2002;224(3):764–8.
11. Gangi S, et al. Time interval between abnormalities seen on CT and the clinical diagnosis of pancreatic cancer: retrospective review of CT scans obtained before diagnosis. *AJR Am J Roentgenol*. 2004;182(4):897–903.
12. Tajima Y, et al. Pancreatic carcinoma coexisting with chronic pancreatitis versus tumor-forming pancreatitis: diagnostic utility of the time-signal intensity curve from dynamic contrast-enhanced MR imaging. *World J Gastroenterol*. 2007;13(6):858–65.
13. Kim T, et al. Pancreatic mass due to chronic pancreatitis: correlation of CT and MR imaging features with pathologic findings. *AJR Am J Roentgenol*. 2001;177(2):367–71.
14. Conwell DL, et al. American pancreatic association practice guidelines in chronic pancreatitis: evidence-based report on diagnostic guidelines. *Pancreas*. 2014;43(8):1143–62.
15. Yadav AK, et al. Perfusion CT: can it predict the development of pancreatic necrosis in early stage

- of severe acute pancreatitis? *Abdom Imaging*. 2015;40(3):488–99.
16. Malka D, et al. Risk of pancreatic adenocarcinoma in chronic pancreatitis. *Gut*. 2002;51(6):849–52.
 17. Perez-Johnston R, Sainani NI, Sahani DV. Imaging of chronic pancreatitis (including groove and autoimmune pancreatitis). *Radiol Clin N Am*. 2012;50(3):447–66.
 18. Worhunsky DJ, et al. Pancreatic neuroendocrine tumours: hypoenhancement on arterial phase computed tomography predicts biological aggressiveness. *HPB (Oxford)*. 2014;16(4):304–11.
 19. Merkle EM, Bender GN, Brambs HJ. Imaging findings in pancreatic lymphoma: differential aspects. *AJR Am J Roentgenol*. 2000;174(3):671–5.
 20. Allen PJ, et al. Multi-institutional validation study of the American Joint Commission on Cancer (8th edition) changes for T and N staging in patients with pancreatic adenocarcinoma. *Ann Surg*. 2017;265(1):185–91.
 21. Saka B, et al. Pancreatic ductal adenocarcinoma is spread to the peripancreatic soft tissue in the majority of resected cases, rendering the AJCC T-stage protocol (7th edition) inapplicable and insignificant: a size-based staging system (pT1: ≤ 2 , pT2: $> 2 - \leq 4$, pT3: > 4 cm) is more valid and clinically relevant. *Ann Surg Oncol*. 2016;23(6):2010–8.
 22. van Roessel S, et al. International validation of the eighth edition of the American joint committee on cancer (AJCC) TNM staging system in patients with resected pancreatic cancer. *JAMA Surg*. 2018;153(12):e183617.
 23. Varadhachary GR, et al. Borderline resectable pancreatic cancer: definitions, management, and role of preoperative therapy. *Ann Surg Oncol*. 2006;13(8):1035–46.
 24. Lu DS, et al. Local staging of pancreatic cancer: criteria for unresectability of major vessels as revealed by pancreatic-phase, thin-section helical CT. *AJR Am J Roentgenol*. 1997;168(6):1439–43.
 25. Wong JC, Lu DS. Staging of pancreatic adenocarcinoma by imaging studies. *Clin Gastroenterol Hepatol*. 2008;6(12):1301–8.
 26. Al-Hawary MM, et al. Pancreatic ductal adenocarcinoma radiology reporting template: consensus statement of the society of abdominal radiology and the american pancreatic association. *Gastroenterology*. 2014;146(1):291–304.e1.
 27. Katz MH, et al. Response of borderline resectable pancreatic cancer to neoadjuvant therapy is not reflected by radiographic indicators. *Cancer*. 2012;118(23):5749–56.
 28. Boellaard R, et al. FDG PET/CT: EANM procedure guidelines for tumour imaging: version 2.0. *Eur J Nucl Med Mol Imaging*. 2015;42(2):328–54.
 29. Kim R, et al. PET/CT fusion scan prevents futile laparotomy in early stage pancreatic cancer. *Clin Nucl Med*. 2015;40(11):e501–5.
 30. Ruan Z, et al. Multi-modality imaging features distinguish pancreatic carcinoma from mass-forming chronic pancreatitis of the pancreatic head. *Oncol Lett*. 2018;15(6):9735–44.
 31. Toft J, et al. Imaging modalities in the diagnosis of pancreatic adenocarcinoma: a systematic review and meta-analysis of sensitivity, specificity and diagnostic accuracy. *Eur J Radiol*. 2017;92:17–23.
 32. Kauhanen SP, et al. A prospective diagnostic accuracy study of 18F-fluorodeoxyglucose positron emission tomography/computed tomography, multidetector row computed tomography, and magnetic resonance imaging in primary diagnosis and staging of pancreatic cancer. *Ann Surg*. 2009;250(6):957–63.
 33. Yeh R, et al. The role of 18F-FDG PET/CT and PET/MRI in pancreatic ductal adenocarcinoma. *Abdom Radiol (NY)*. 2018;43(2):415–34.
 34. Wang Z, et al. FDG-PET in diagnosis, staging and prognosis of pancreatic carcinoma: a meta-analysis. *World J Gastroenterol*. 2013;19(29):4808–17.
 35. Crippa S, et al. The role of (18)fluoro-deoxyglucose positron emission tomography/computed tomography in resectable pancreatic cancer. *Dig Liver Dis*. 2014;46(8):744–9.
 36. Wang S, et al. The value of (18)F-FDG PET/CT and carbohydrate antigen 19-9 in predicting lymph node micrometastases of pancreatic cancer. *Abdom Radiol (NY)*. 2019;44(12):4057–62.
 37. Zhu D, et al. Prognostic value of 18F-FDG-PET/CT parameters in patients with pancreatic carcinoma: a systematic review and meta-analysis. *Medicine (Baltimore)*. 2017;96(33):e7813.
 38. Rayamajhi S, et al. Utility of (18) F-FDG PET/CT and CECT in conjunction with serum CA 19-9 for detecting recurrent pancreatic adenocarcinoma. *Abdom Radiol (NY)*. 2018;43(2):505–13.
 39. Ly JN, Miller FH. MR imaging of the pancreas: a practical approach. *Radiol Clin N Am*. 2002;40(6):1289–306.
 40. Miller FH, Rini NJ, Kepcke AL. MRI of adenocarcinoma of the pancreas. *AJR Am J Roentgenol*. 2006;187(4):W365–74.
 41. Obuz F, et al. Pancreatic adenocarcinoma: detection and staging with dynamic MR imaging. *Eur J Radiol*. 2001;38(2):146–50.
 42. Manfredi R, et al. Severe chronic pancreatitis versus suspected pancreatic disease: dynamic MR cholangiopancreatography after secretin stimulation. *Radiology*. 2000;214(3):849–55.
 43. Balthazar EJ. Pancreatitis associated with pancreatic carcinoma. Preoperative diagnosis: role of CT imaging in detection and evaluation. *Pancreatol*. 2005;5(4–5):330–44.
 44. Jenkins JP, et al. Quantitative tissue characterisation in pancreatic disease using magnetic resonance imaging. *Br J Radiol*. 1987;60(712):333–41.
 45. Ichikawa T, et al. Duct-penetrating sign at MRCP: usefulness for differentiating inflammatory pancreatic mass from pancreatic carcinomas. *Radiology*. 2001;221(1):107–16.
 46. Siddiqi AJ, Miller F. Chronic pancreatitis: ultrasound, computed tomography, and magnetic reso-

- nance imaging features. *Semin Ultrasound CT MR*. 2007;28(5):384–94.
47. Lopez Hanninen E, et al. Prospective evaluation of pancreatic tumors: accuracy of MR imaging with MR cholangiopancreatography and MR angiography. *Radiology*. 2002;224(1):34–41.
 48. Fayad LM, Mitchell DG. Magnetic resonance imaging of pancreatic adenocarcinoma. *Int J Gastrointest Cancer*. 2001;30(1–2):19–25.
 49. Adamek HE, et al. Pancreatic cancer detection with magnetic resonance cholangiopancreatography and endoscopic retrograde cholangiopancreatography: a prospective controlled study. *Lancet*. 2000;356(9225):190–3.
 50. Matsuki M, et al. Diffusion-weighted MR imaging of pancreatic carcinoma. *Abdom Imaging*. 2007;32(4):481–3.
 51. Kim JK, et al. Focal pancreatic mass: distinction of pancreatic cancer from chronic pancreatitis using gadolinium-enhanced 3D-gradient-echo MRI. *J Magn Reson Imaging*. 2007;26(2):313–22.
 52. Schima W, et al. Pancreatic adenocarcinoma. *Eur Radiol*. 2007;17(3):638–49.
 53. Danet IM, et al. Liver metastases from pancreatic adenocarcinoma: MR imaging characteristics. *J Magn Reson Imaging*. 2003;18(2):181–8.
 54. Pamuklar E, Semelka RC. MR imaging of the pancreas. *Magn Reson Imaging Clin N Am*. 2005;13(2):313–30.
 55. Horvat N, et al. Subclinical focal cholangitis mimicking liver metastasis in asymptomatic patients with history of pancreatic ductal adenocarcinoma and biliary tree intervention. *Cancer Imaging*. 2017;17(1):21.
 56. Scialpi M, et al. Imaging evaluation of post pancreatic surgery. *Eur J Radiol*. 2005;53(3):417–24.